

# A Secure Network Coding based Image Communications in Two-Hop Wireless Relay Networks

Quoc-Tuan Vien<sup>†</sup> and Tuan T. Nguyen<sup>‡</sup>

<sup>†</sup>Faculty of Science and Technology, Middlesex University, UK. Email: Q.Vien@mdx.ac.uk.

<sup>‡</sup>School of Computing and Mathematical Sciences, University of Greenwich, UK. Email: Tuan.Nguyen@greenwich.ac.uk.

**Abstract**—This paper investigates the image communications in two-hop wireless relay networks (TH-WRNs) where a source node sends images to a destination node with the assistance of a relay node via two hops, i.e. source-to-relay and relay-to-destination links. Due to the broadcast nature of wireless media, there exists an eavesdropper who tries to overhear and recover the images. Aiming to enhance the security and also to save transmission bandwidth of the image communications, we propose a secure relaying transmission (SRT) protocol by exploiting both random linear network coding (RLNC) and image super-resolution (ISR) techniques. In the proposed protocol, the original high-resolution (HR) images are downscaled at the source node and the RLNC is employed at both the source and relay nodes to conceal the original images from the eavesdropper. The RLNC decoding and ISR are adopted at the destination node to decode and recover the HR images, while the eavesdropper cannot decode the images due to the unawareness of the coefficient matrices and the reference images in the RLNC. It is shown that the proposed SRT protocol achieves a significantly higher performance at the destination than at the eavesdropper. Furthermore, with high-quality relaying hops, the SRT protocol outperforms the secure direct transmission (SDT) protocol with only a direct link between the source and the destination nodes. Finally, simulation results are provided to verify the findings.

**Index Terms**—Image super-resolution; Deep Learning; Random linear network coding; Wireless relay networks

## I. INTRODUCTION

The communications between two end nodes can be realised with the assistance of intermediate nodes, a.k.a. relay nodes, via two hops: source-to-relay and relay-to-destination. The relay nodes in two-hop wireless relay networks (TH-WRNs) do not simply store the data received from source nodes, but they can process the data prior to forward to destination nodes. Specifically, network coding (NC) [1] has been applied at the relay nodes to improve network throughput [2] by performing linear NC (RLNC) on the data packets from the source nodes. Following random linear NC (RLNC) approach, a secure NC was proposed in [3] to enhance the security of wiretap channels where the relay nodes randomly and linearly combine the decoded data with the encrypted key prior to forwarding to destination nodes.

Considering image communications over TH-WRNs, the conventional relaying protocols can be adopted; however, there exist several issues related to data privacy and transmission bandwidth, which should be taken into account. Image super resolution (ISR) has been employed to recover high-resolution

(HR) images from their low-resolution (LR) versions [4], [5]. Specifically, very deep super resolution (VDSR) was shown to provide a high performance with a high running speed [6].

Inspired by RLNC and ISR, this paper proposes a secure relaying transmission (SRT) protocol to not only conceal the image, but also save the transmission bandwidth of the image communications in the TH-WRNs. In the proposed scheme, the original HR images at source node are firstly downscaled to save the transmission bandwidth. The LR images are then combined with reference images by the RLNC encoding to conceal the original images from an eavesdropper. At relaying node, the received images are denoised and decoded by using the shared reference images from Alica along with the RLNC coefficients. Then, the relay mixes the decoded images with different reference images prior to forwarding to destination node. Given the shared reference images, the destination can perform the RLNC decoding and employ the ISR to recover the original HR images. Meanwhile, without knowledge of the RLNC coefficients and reference images, the eavesdropper cannot decode any images from both the source and relay nodes.

The performance of the proposed SRT protocol is evaluated and compared with that of secure direct transmission (SDT) protocol which consists only a direct link between source and destination nodes. It is shown that both protocols achieve a higher peak signal-to-noise ratio (PSNR) at the destination node than eavesdropper, especially when the eavesdropper is not aware of the reference images at the source and relay nodes. Moreover, the SRT protocol is shown to outperform the SDT protocol given a high quality of the relaying links, while the SDT protocol is superior when the direct link is of higher quality compared to the relaying links. This accordingly verifies the benefit of employing the relay in the proposed SRT protocol for not only extending the coverage due to the missing of the direct link, but also providing an enhanced performance.

## II. SYSTEM MODEL

Figure 1 illustrates a typical TH-WRN in which Alice  $\mathcal{A}$  wishes to send an image to Bob  $\mathcal{B}$  with the assistance of a relay  $\mathcal{R}$ . It is assumed there is no direct link between  $\mathcal{A}$  and  $\mathcal{B}$  due to either environmental limitations with obstacles or limited transmission power, and thus  $\mathcal{R}$ , which is located in between  $\mathcal{A}$  and  $\mathcal{B}$ , is exploited to assist the image communications.

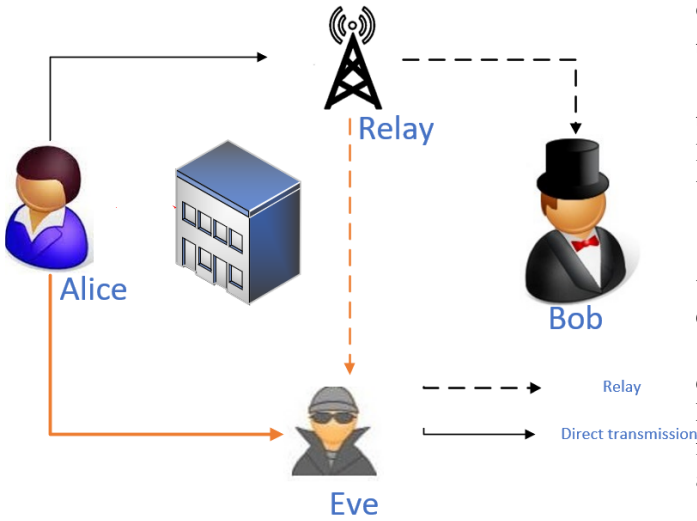


Fig. 1: System model of a typical TH-WRN.

Along with the licenced users, there exists an eavesdropper  $\mathcal{E}$  who tries to overhear the data from both  $\mathcal{A}$  and  $\mathcal{R}$ .

Over the air, it is assumed the image communication link between any pair of nodes  $\mathcal{X}$  and  $\mathcal{Y}$ ,  $\{\mathcal{X}, \mathcal{Y}\} \in \{\mathcal{A}, \mathcal{B}, \mathcal{R}, \mathcal{E}\}$ , experiences an additive white Gaussian noise (AWGN). Colour images are considered, which can be represented as  $M \times N \times 3$  arrays.

In the proposed SRT protocol, the image communications between  $\mathcal{A}$  and  $\mathcal{B}$  can be realised in two time slots:  $\mathcal{A}$  sends the RLNC-encoded image to  $\mathcal{R}$  in the first time slot and then  $\mathcal{R}$  decodes the received image, performs RLNC encoding and forwards the encoded image to  $\mathcal{B}$  in the second time slot. Meanwhile,  $\mathcal{E}$  can overhear and try to decode the images in both time slots from  $\mathcal{A}$  and  $\mathcal{R}$  using the wiretap links.

### III. PROPOSED SRT PROTOCOL IN TH-WRNs

In the proposed SRT protocol, the image processing with encoding and decoding is adopted in the communications to not only enhance the security, but also save the bandwidth of the image transmission between  $\mathcal{A}$  and  $\mathcal{B}$  over TH-WRNs.

The original image at  $\mathcal{A}$ , i.e.  $\mathbf{I}_{\mathcal{A}}^{(HR)}$  of size  $M \times N \times 3$ , is firstly downsampled with bicubic interpolation and scaling factor  $\epsilon$ . Its LR version is given by  $\mathbf{I}_{\mathcal{A}}^{(LR)}$  of size  $M' \times N' \times 3$ , where  $M' = \lceil M/\epsilon \rceil$ ,  $N' = \lceil N/\epsilon \rceil$  and  $\lceil x \rceil \triangleq \arg \min_{n \in \mathbb{Z}} n \geq x$ . Then, RLNC is applied at  $\mathcal{A}$  to mix  $\mathbf{I}_{\mathcal{A}}^{(LR)}$  with a reference image, denoted by  $\mathbf{I}_{\mathcal{A}}^{(ref)}$ , which is randomly selected from a shared image datastore  $\mathcal{S}$  accessible to legitimate users, i.e.  $\mathcal{A}$ ,  $\mathcal{R}$  and  $\mathcal{B}$ . The encoded image at  $\mathcal{A}$  can be written by

$$\mathbf{I}_{\mathcal{A}}^{(enc)} = \mathbf{M}_{\mathcal{A},1} \circ \mathbf{I}_{\mathcal{A}}^{(LR)} + \mathbf{M}_{\mathcal{A},2} \circ \mathbf{I}_{\mathcal{A}}^{(ref)}, \quad (1)$$

where  $\mathbf{M}_{\mathcal{A},k}$ ,  $k \in \{1, 2\}$ , of size  $M' \times N' \times 3$  are RLNC coefficient matrices at  $\mathcal{A}$  and  $\circ$  denotes the element-wise multiplication of two matrices. Let  $\alpha_{\mathcal{A},m,n,p}^{(k)}$ ,  $m \in \{1, 2, \dots, M'\}$ ,  $n \in \{1, 2, \dots, N'\}$ ,  $p \in \{1, 2, 3\}$  denote the coefficient in matrix  $\mathbf{M}_{\mathcal{A},k}$ . In order to restrict the value of the image pixels

of the encoded image not exceeding its range,  $\alpha_{\mathcal{A},m,n,p}^{(k)}$  is in the range  $[0, 1]$  and  $\alpha_{\mathcal{A},m,n,p}^{(1)} + \alpha_{\mathcal{A},m,n,p}^{(2)} = 1$ .

The RLNC-encoded image  $\mathbf{I}_{\mathcal{A}}^{(enc)}$  is then forwarded to  $\mathcal{R}$  in the form of a modulated data packet, denoted by  $\mathbf{x}_{\mathcal{A}}$ , over the legitimate wireless channels. The received signals at  $\mathcal{R}$  can be written by

$$\mathbf{r}_{\mathcal{R}} = \mathbf{x}_{\mathcal{A}} + \mathbf{n}_{\mathcal{R}}, \quad (2)$$

where  $\mathbf{n}_{\mathcal{R}}$  is an independent AWGN vector at  $\mathcal{R}$  with each entry having zero mean and variance of  $\sigma_{\mathcal{R}}^2$ .

Receiving the data from  $\mathcal{A}$ , the relay  $\mathcal{R}$  firstly decodes the data as  $\hat{\mathbf{x}}_{\mathcal{R}}$  and then denoise the image using a pretrained DnCNN network [7] as  $\bar{\mathbf{I}}_{\mathcal{R}}$ . Using the shared reference image from  $\mathcal{A}$ , i.e.  $\mathbf{I}_{\mathcal{A}}^{(ref)}$ , and RLNC coefficient matrices, i.e.  $\mathbf{M}_{\mathcal{A},1}$  and  $\mathbf{M}_{\mathcal{A},2}$ , the original image can be decoded at  $\mathcal{R}$  as

$$\hat{\mathbf{I}}_{\mathcal{R}} = \left( \bar{\mathbf{I}}_{\mathcal{R}} - \mathbf{M}_{\mathcal{A},2} \circ \mathbf{I}_{\mathcal{A}}^{(ref)} \right) \oslash \mathbf{M}_{\mathcal{A},1}, \quad (3)$$

where  $\oslash$  denotes the element-wise division of two matrices.

Following RLNC method,  $\mathcal{R}$  encodes the recovered image from  $\mathcal{A}$ , i.e.  $\hat{\mathbf{I}}_{\mathcal{R}}^{(1)}$ , by mixing it with a reference image, denoted by  $\mathbf{I}_{\mathcal{R}}^{(ref)}$ ,<sup>1</sup> as follows:

$$\mathbf{I}_{\mathcal{R}}^{(enc)} = \mathbf{M}_{\mathcal{R},1} \circ \hat{\mathbf{I}}_{\mathcal{R}} + \mathbf{M}_{\mathcal{R},2} \circ \mathbf{I}_{\mathcal{R}}^{(ref)}, \quad (4)$$

where  $\mathbf{M}_{\mathcal{R},k}$ ,  $k \in \{1, 2\}$ , of size  $M' \times N' \times 3$  are RLNC coefficient matrices at  $\mathcal{R}$ .

In the second time slot,  $\mathcal{R}$  forwards the encoded image  $\mathbf{I}_{\mathcal{R}}^{(enc)}$  to  $\mathcal{B}$  in the form of a modulated data packet, denoted by  $\mathbf{x}_{\mathcal{R}}$ . The received signal at  $\mathcal{B}$  can be written by

$$\mathbf{r}_{\mathcal{B}} = \mathbf{x}_{\mathcal{R}} + \mathbf{n}_{\mathcal{B}}, \quad (5)$$

where  $\mathbf{n}_{\mathcal{B}}$  is an AWGN vector at  $\mathcal{B}$  with each entry having zero mean and variance of  $\sigma_{\mathcal{B}}^2$ .

Similarly,  $\mathcal{B}$  decodes the data received from  $\mathcal{A}$  as  $\hat{\mathbf{x}}_{\mathcal{B}}$  and denoises the image using the pretrained DnCNN network as  $\bar{\mathbf{I}}_{\mathcal{B}}$ . Then,  $\mathcal{B}$  recovers the image transmitted from  $\mathcal{R}$  using RLNC decoding as follows:

$$\hat{\mathbf{I}}_{\mathcal{B}} = \left( \bar{\mathbf{I}}_{\mathcal{B}} - \mathbf{M}_{\mathcal{R},2} \circ \mathbf{I}_{\mathcal{R}}^{(ref)} \right) \oslash \mathbf{M}_{\mathcal{R},1}. \quad (6)$$

It is worth noticing that the reference image and the RLNC coefficient matrices employed for RLNC encoding at  $\mathcal{R}$  are shared with  $\mathcal{B}$  to be able to recover the image.

Employing ISR framework,  $\mathcal{B}$  can recover the full size of the original image transmitted from  $\mathcal{A}$ , denoted by  $\hat{\mathbf{I}}_{\mathcal{B}}^{(HR)}$ , as

$$\hat{\mathbf{I}}_{\mathcal{B}}^{(HR)} = \nabla_{\epsilon}(\hat{\mathbf{I}}_{\mathcal{B}}), \quad (7)$$

where  $\nabla_{\epsilon}(\cdot)$  denotes the ISR operator to reconstruct the upsampled images with scaling factor  $\epsilon$ .

<sup>1</sup>The reference image  $\mathbf{I}_{\mathcal{R}}^{(ref)}$  at  $\mathcal{R}$  is different from that at  $\mathcal{A}$ , though it is also randomly selected from the same image datastore  $\mathcal{S}$  shared between the legitimate users.

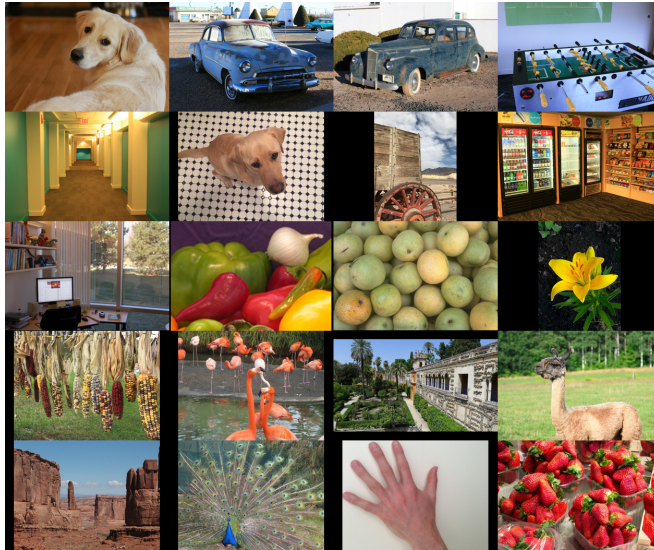


Fig. 2: Images for testing and validation of the proposed cooperative secure image super-resolution.

#### Image Decoding and Estimation at Eve:

Over the wireless media,  $\mathcal{E}$  can overhear the data packets transmitted from both  $\mathcal{A}$  and  $\mathcal{R}$  although that they are not intended for him. Following the same decoding approach,  $\mathcal{E}$  tries to decode the data from  $\mathcal{A}$  and  $\mathcal{R}$  as  $\hat{\mathbf{x}}_{\mathcal{E}}^{(1)}$  and  $\hat{\mathbf{x}}_{\mathcal{E}}^{(2)}$ , respectively. Deep neural network with a pretrained DnCNN network is also employed to denoise both images as  $\bar{\mathbf{I}}_{\mathcal{E}}^{(1)}$  and  $\bar{\mathbf{I}}_{\mathcal{E}}^{(2)}$ .

However,  $\mathcal{E}$  does not know the reference images, i.e.  $\mathbf{I}_{\mathcal{A}}^{(ref)}$  and  $\mathbf{I}_{\mathcal{R}}^{(ref)}$ , in the image datastore, which is only shared between the legitimate users, along with RLNC coefficient matrices, i.e.  $\{\mathbf{M}_{\mathcal{A},1}, \mathbf{M}_{\mathcal{A},2}\}$  and  $\{\mathbf{M}_{\mathcal{R},1}, \mathbf{M}_{\mathcal{R},2}\}$ , which are used at  $\mathcal{A}$  and  $\mathcal{R}$  for concealing the original image. In order to recover the images,  $\mathcal{E}$  can make an estimate of the RLNC coefficient matrices and the reference images in the datastore.

#### IV. SIMULATION RESULTS

This section presents the simulation results of the proposed SRT protocol for secure image communications in TH-WRNs. PSNR is used to measure the quality of the recovered image at  $\mathcal{B}$ , i.e.  $\hat{\mathbf{I}}_{\mathcal{B}}^{(HR)}$ , with respect to the HR image transmitted from  $\mathcal{A}$ , i.e.  $\mathbf{I}_{\mathcal{A}}^{(HR)}$ . The simulation is carried out in MATLAB where an image dataset of 20,000 still natural images in the IAPR TC-12 benchmark [8] is selected for training with scaling factors  $\epsilon \in \{4, 6, 8, 10\}$ , and undistorted images from the Image Processing Toolbox (as shown in Fig. 2) are used for validation. In the following, the performance of the SRT protocol is compared with that of the SDT protocol having only a direct  $\mathcal{A}$ - $\mathcal{B}$  link.

Figure 3 plots the PSNR of SRT and SDT protocols as a function of the noise variance of the direct  $\mathcal{A}$  -  $\mathcal{B}$  link in the first time slot, i.e.  $\sigma_{\mathcal{B},1}^2$ . It is assumed that  $\mathcal{R}$  is located

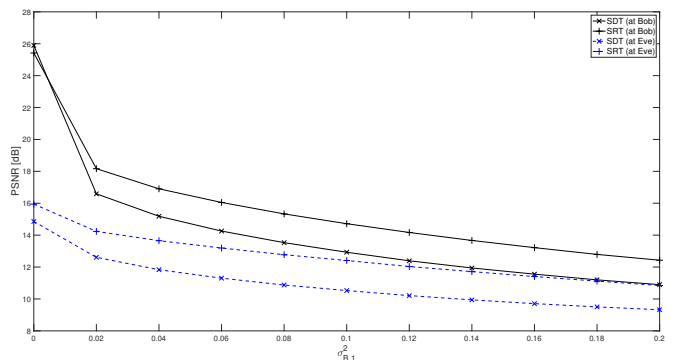


Fig. 3: PSNR of SRT and SDT protocols.

in between  $\mathcal{A}$  and  $\mathcal{B}$ , where the relaying links experience the same noise variance, which is equal to half of the noise variance of the direct link, i.e.  $\sigma_{\mathcal{R}}^2 = \sigma_{\mathcal{B}}^2 = \sigma_{\mathcal{B},1}^2/2$ . The noise variances of the wiretap links are assumed to be the same as those of relaying links, i.e.  $\sigma_{\mathcal{E},1}^2 = \sigma_{\mathcal{R}}^2$  and  $\sigma_{\mathcal{E},2}^2 = \sigma_{\mathcal{B}}^2$ . The original HR images are first downscaled at  $\mathcal{A}$  by four times, i.e.  $\epsilon = 4$ , prior to transmission. For encoding at  $\mathcal{A}$  and  $\mathcal{R}$ , the elements in RLNC matrices are supposed to be in the range  $[0.3, 0.5]$  and known to  $\mathcal{B}$ . In Fig. 3,  $\mathcal{E}$  is assumed to be aware of the reference images used for the RLNC encoding. Both protocols are shown to achieve a better performance at Bob of up to 8 dB in the PSNR than that at Eve since Eve does not know the RLNC coefficient matrices at Alice and Bob. In particular, with the assistance of  $\mathcal{R}$ , an enhanced performance is obtained with the SRT protocol compared to the SDT protocol.

The effectiveness of the proposed protocol is further illus-

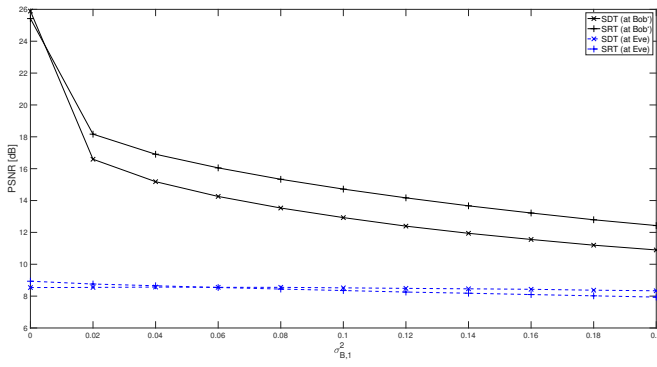


Fig. 4: PSNR of SRT and SDT protocols with incorrect  $\hat{\mathbf{I}}_{\mathcal{A}}^{(ref)}$  and  $\hat{\mathbf{I}}_{\mathcal{R}}^{(ref)}$ .

trated in Fig. 4 where the PSNR of SRT and SDT protocols are plotted versus the noise variance  $\sigma_{\mathcal{B},1}^2$  of the direct  $\mathcal{A} - \mathcal{B}$  link when the reference images are incorrectly estimated at  $\mathcal{E}$ , i.e.  $\hat{\mathbf{I}}_{\mathcal{A}}^{(ref)}$  and  $\hat{\mathbf{I}}_{\mathcal{R}}^{(ref)}$ . It can be observed that a significantly enhanced performance is achieved at  $\mathcal{B}$  compared to  $\mathcal{E}$  due to the incorrect reference image estimated at  $\mathcal{E}$ . This accordingly verifies the effectiveness of the SRT protocol in providing a secure image communications in TH-WRNs.

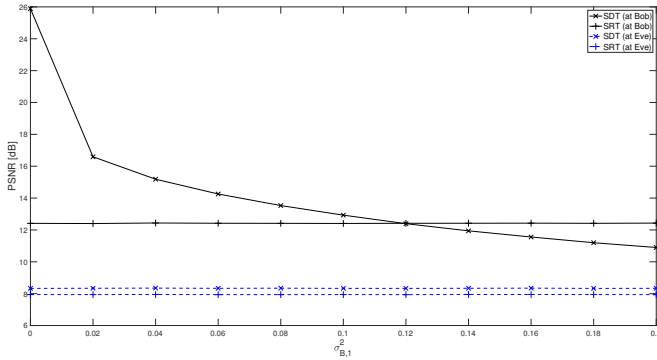


Fig. 5: PSNR versus noise variance of Alice-Bob link.

Taking into account the direct link in TH-WRNs, Fig. 5 plots the PSNR versus  $\sigma_{\mathcal{B},1}^2$ , where the noise variances of other links are fixed as  $\sigma_{\mathcal{R}}^2 = \sigma_{\mathcal{B}}^2 = 0.1$ ,  $\sigma_{\mathcal{E},1}^2 = 0.2$  and  $\sigma_{\mathcal{E},2}^2 = 0.1$ , respectively. It can be observed that the SRT is better than the SDT protocol at high  $\sigma_{\mathcal{B},1}^2$ , while the SDT outperforms the SRT protocol at low  $\sigma_{\mathcal{B},1}^2$ . This reflects the practical scenario that the usage of relay is not always necessary, especially when the direct link is already of good quality.

The impacts of relaying links, i.e.  $\mathcal{A} - \mathcal{R}$  and  $\mathcal{R} - \mathcal{B}$  links, are shown in Figs. 6 and 7, where the PSNR is plotted versus  $\sigma_{\mathcal{R}}^2$  and  $\sigma_{\mathcal{B}}^2$ , respectively. It is assumed that  $\sigma_{\mathcal{B}}^2 = 0.1$  in Fig. 6, while  $\sigma_{\mathcal{R}}^2 = 0.1$  dB in Fig. 7. In both figures, the noise variances of other links are  $\sigma_{\mathcal{B},1}^2 = 0.2$ ,  $\sigma_{\mathcal{E},1}^2 = 0.2$  and  $\sigma_{\mathcal{E},2}^2 = 0.1$ . It can be observed that a better performance is achieved with the proposed SRT protocol over the whole

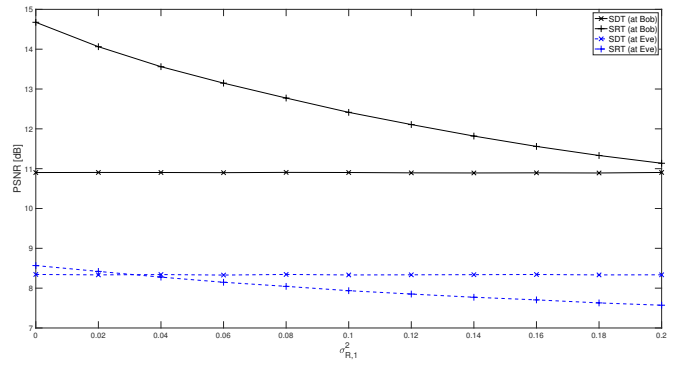


Fig. 6: PSNR versus noise variance of Alice-Relay link.

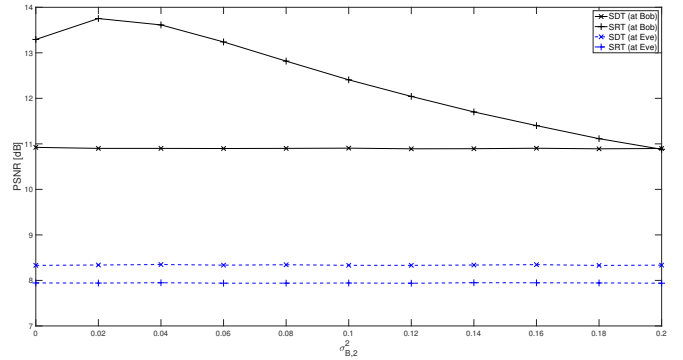


Fig. 7: PSNR versus noise variance of Relay-Bob link.

range of  $\sigma_{\mathcal{R}}^2$  and  $\sigma_{\mathcal{B}}^2$ . Meanwhile, the SDT scheme is shown to be independent of the quality of the relaying links as  $\mathcal{R}$  is not involved in communications between  $\mathcal{A}$  and  $\mathcal{B}$ .

## V. CONCLUSIONS

In this paper, we have proposed an SRT protocol for image communications in TH-WRNs where Alice wishes to securely transfer HR images to Bob with the assistance of a relay via two hops. RLNC has been employed at Alice and the relay to conceal the original images from Eve. Also, ISR has been applied to recover the HR images at Bob from their LR versions which were downscaled at Alice prior to transmit to Relay. It has been shown that the proposed SRT protocol achieves a higher PSNR at Bob compared to that at Eve. Investigating the impacts of communication links, it has been demonstrated that the relay is only necessary when the direct Alice-Bob link experience high noise and relaying links are critical in the SRT protocol. In particular, given lack of knowledge of RLNC coefficient matrices used at Alice and the relay along with reference images in the shared image datastore, Eve can not decode the original HR images, even with high-quality wiretap links and ISR. This accordingly verifies the effectiveness of the proposed SRT protocol in securing the transmission of the original HR images with a low transmission bandwidth in the TH-WRNs.

## REFERENCES

- [1] R. Ahlswede, N. Cai, S.-Y. Li, and R. Yeung, "Network information flow," *IEEE Transactions on Information Theory*, vol. 46, no. 4, pp. 1204–1216, 2000.
- [2] R. Louie, Y. Li, and B. Vucetic, "Practical physical layer network coding for two-way relay channels: Performance analysis and comparison," *IEEE Trans. Wireless Commun.*, vol. 9, no. 2, pp. 764–777, Feb. 2010.
- [3] T. Cui, T. Ho, and J. Kliewer, "On secure network coding with nonuniform or restricted wiretap sets," *IEEE Trans. Inf. Theory*, vol. 59, no. 1, pp. 166–176, Jan. 2013.
- [4] Z. Wang, J. Chen, and S. C. H. Hoi, "Deep learning for image super-resolution: A survey," *IEEE Trans. Pattern Anal. Mach. Intell.*, pp. 1–1, 2020.
- [5] Y. K. Ooi and H. Ibrahim, "Deep learning algorithms for single image super-resolution: A systematic review," *Electronics*, vol. 10, no. 7, 2021. [Online]. Available: <https://www.mdpi.com/2079-9292/10/7/867>
- [6] J. Kim, J. Kwon Lee, and K. Mu Lee, "Accurate image super-resolution using very deep convolutional networks," in *Proceedings of the IEEE conference on computer vision and pattern recognition*, 2016, pp. 1646–1654.
- [7] K. Zhang, W. Zuo, Y. Chen, D. Meng, and L. Zhang, "Beyond a Gaussian denoiser: Residual learning of deep CNN for image denoising," *IEEE Trans. Image Process.*, vol. 26, no. 7, pp. 3142–3155, 2017.
- [8] M. Grubinger, P. D. Clough, H. Müller, and T. Deselaers, "The IAPR TC-12 benchmark: A new evaluation resource for visual information systems," 2006.